The Egyptian Journal of Remote Sensing and Space Sciences (2016) 19, 207–222

HOSTED BY

ELSEVIER

National Authority for Remote Sensing and Space Sciences

The Egyptian Journal of Remote Sensing and Space Sciences

www.elsevier.com/locate/ejrs
www.sciencedirect.com

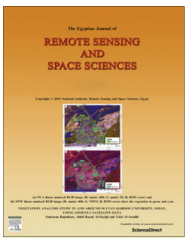

RESEARCH PAPER

Remotely sensed data capacities to assess soil degradation

Behzad Rayegani [a,*], **Susan Barati** [b], **Tayebeh Alsadat Sohrabi** [c], **Bahareh Sonboli** [a]

[a] *Department of Environmental Sciences and Natural Resources, University of Environment, Karaj, Iran*
[b] *Faculty of Natural Resources, Isfahan University of Technology, Isfahan, Iran*
[c] *Faculty of Natural Resources & Earth Science, Kashan University, Kashan, Iran*

Received 4 August 2015; revised 16 October 2015; accepted 14 December 2015
Available online 7 January 2016

KEYWORDS

Iranian Model of Desertification Potential Assessment;
LADA methodology of land degradation;
Remote sensed time series;
Artificial neural networks

Abstract This research has tried to take advantage of the two-field based methodology in order to assess remote sensing data capacities for modeling soil degradation. Based on the findings of our investigation, preprocessing analysis types have not shown significant effects on the accuracy of the model. Conversely, type of indicators and indices of the used field based model has a large impact on the accuracy of the model. In addition, using some remote sensed indices such as iron oxide index and ferrous minerals index can help to improve modeling accuracy of some field indices of soil condition assessment. According to the results, the model capacities can significantly be improved by using time-series remotely sensed data compared with using single date data. In addition, if artificial neural networks are used on single remotely sensed data instead of multivariate linear regression, accuracy of the model can be increased dramatically because it helps the model to take the nonlinear form. However, if time series of remotely sensed data are used, the accuracy of the artificial neural network modeling is not much different from the accuracy of the regression model. It turned out to be contrary to what is thought, but according to our results, increasing the number of inputs to artificial neural network modeling in practice reduces the actual accuracy of the model.

1. Introduction

Land degradation or desertification is very important due to its impact on the loss of productivity or economic power. This degradation includes three main aspects as follows: (1) soil degradation, (2) water degradation, and (3) vegetation degradation (de Paz et al., 2006; McDonagh and Bunning, 2009a).

Soil degradation has been considered as one of the three main components of land degradation and efforts have been done to determine its relationship with desertification for more than two decades. Since the soil is considered as a renewable source (de Paz et al., 2006), its degradation is a major threat in the entire world and in the long-term leads to soil productivity deficiency and environmental instability (Diodato and

* Corresponding author. Tel.: +98 263 280 7445, cell: +98 913 304 4086.
E-mail address: bhz.ray@gmail.com (B. Rayegani).

Peer review under responsibility of National Authority for Remote Sensing and Space Sciences.

http://dx.doi.org/10.1016/j.ejrs.2015.12.001

Ceccarelli, 2004). Therefore, assessing the conditions of soil is needed for understanding the current status (Snakin et al., 1996).

Each aspect of soil degradation has different evidences and subsets, and the indices and indicators have been proposed to identify and evaluate them. So far, many attempts have been made to collect indicators of soil degradation in the form of a model and several methods have been proposed for the assessment of soil degradation phenomena (Abdel Kawy and Belal, 2011; Abdel Kawy and Ali, 2012; Cammeraat and Imeson, 1998; de Paz et al., 2006; Diodato and Ceccarelli, 2004; El Baroudy and Moghanm, 2014; McDonagh and Bunning, 2009a; Omuto, 2008; Rasmy et al., 2010; Rodríguez et al., 2005; Ruiz-Sinoga and Diaz, 2010; Sha-Sha et al., 2011; Snakin et al., 1996; Stocking and Murnaghan, 2000; Yanda, 2000).

However, perhaps three methodologies can be distinguished to evaluate land degradation due to their widespread exploitation in comparison to other models which are considered as soil quality criteria:

(1) The provisional methodology for assessing and mapping of desertification: It was formulated by FAO and UNEP. It is the first method in the evaluation and mapping of desertification developed by FAO and UNEP (FAO/UNEP, 1983). In this method, seven processes have been considered in land degradations. The six types of processes associated with soil degradation.
(2) Methodology for mapping Environmentally Sensitive Areas (ESAs) to desertification or methods provided by project MEDALUS: In this method, a variety of ESAs to desertification can be recognized by using the special key (main) criteria and the mapped method. These criteria measure the ability of land to withstand more degradation, or show how much land is appropriate for a particular use. In addition, in order to desertification, the key (main) criteria for defining ESAs are classified in four groups of soil quality, climate quality, vegetation quality and management quality (Kosmas et al., 1999).
(3) LADA guideline for land degradation assessment at the local scale. According to the methodology of LADA, land degradation has been assessed in three sections soil, water, and vegetation degradation (McDonagh and Bunning, 2009a,b).

In Iran, based on local and regional needs, Iranian Model of Desertification Potential Assessment (IMDPA) has been created in 2005 with the optimization of the ESAs model (Ahmadi, 2005). In this model, nine different indices have been proposed for potential desertification assessment: (1) climate, (2) geology-geomorphology, (3) soil, (4) vegetation, (5) agriculture, (6) water (7) erosion; (8) socioeconomic, and (9) technology and urban development. In this model, three to four indicators for each criterion have been suggested, for example, soil index composed of texture, depth, salinity and gravel percent indicators.

In all these models, assessment has been carried out on the basis of the field studies and the present situation scoring. But generally the field methods are more time-consuming and don't have necessary standards for being up to date, can't be generalizable to other areas and given similar results at renewing operations, and are the most costly in large areas. While traditional approaches see this kind of measure as incorrect and the most costly, aerial photography and satellite remote sensing systems have considerable advantages in this area. These data cover the entire land and provide reproducible, targeted and summarized data in different spectrums and wavelengths, so they are perfectly appropriate to assess and monitor environmental conditions in arid zones (Pinet et al., 2006). Therefore, the current efforts to survey and assess the state of soil quality have greater emphasis on the remotely sensed techniques than field studies.

Many researchers have tried to analyze soil and land degradation through empirical methods and models (Geist and Lambin, 2004; Ladisa et al., 2012; Liu et al., 2003; Yang et al., 2005), and remotely sensed methods (El Baroudy and Moghanm, 2014; Haijiang et al., 2008; Helldén and Tottrup, 2008; Hill et al., 2008; Rasmussen et al., 2001; Rasmy et al., 2010) and modeling (Feoli et al., 2002; Ibáñez et al., 2008; Jauffret and Visser, 2003; Okin et al., 2009; Ravi et al., 2010; Salvati and Zitti, 2009; Santini et al., 2010; Zucca et al., 2009).

Most of the environmental phenomenon has been examined in the context of two scenarios (Wang et al., 2010): (a) a single-criteria scenario, and (b) a multi-criteria scenario (Ghadiry et al., 2012). Assessment of soil degradation studies can be clearly seen in both scenarios. However, most of the remote sensing studies and the researches about investigation of soil condition have used the single criteria, also multi criteria studies haven't been seen in the form of a model. Numerous studies have been done on the detection of soil salinity using remote sensing (Abdel Kawy and Ali, 2012; Douaoui et al., 2006; Gutierrez and Johnson, 2010; Masoud, 2014; Metternicht and Zinck, 2008; Wang et al., 2013) and a large number of soil quality studies focused on soil chemical factors have been conducted using remote sensing (Abdel Kawy and Belal, 2011; Abdel Kawy and Ali, 2012; Bouaziz et al., 2011; El Baroudy and Moghanm, 2014). But remote sensed investigation of other criteria related to the soil such as organic carbon (Huang et al., 2007), chemical composition (Dogan, 2009; Wang et al., 2013), bare soils distinguish from each other (Zhao and Chen, 2005) and humidity (Goodwin et al., 2008) has been studied extensively.

However, yet there isn't a multi-criteria remotely sensed model of soil degradation that can be accepted by all experts. Therefore, this study has tried to take advantage of the two-field models to assess the ability of remote sensing data in the modeling of soil degradation. In this study, we attempted to investigate the performance of the remote sensing data and answered the follow questions: How much accuracy will the data obtain to provide soil degradation maps using remote sensing? What kinds of remote sensing data should be used in these studies? Single date data are more accurate or time series data? How much can we enhance the modeling accuracy by the nonlinearity of the model?

2. Methodology

2.1. The study area

The study area with a total area of 345,591 hectares is located in the east of Esfahan Province between longitude E 51°56′29″ to E 52°42′22″ and latitude N 32°09′41″ to N 33°03′05″

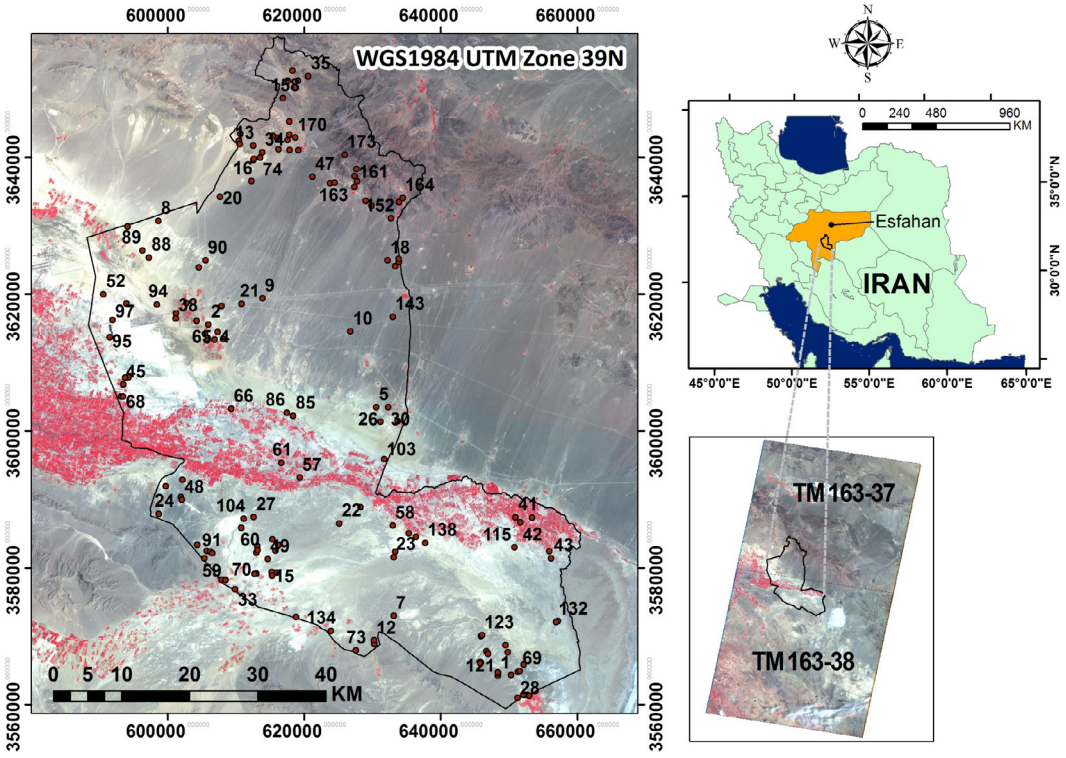

Figure 1 Location of the study area in Esfahan Province, TM Scenes & sample site locations.

(Fig. 1). The elevation of the study area ranges between 1100 m in the south to 3500 m in the north east of the mountains of the area. A large part of the study area has an average altitude of 1400 meters. The average annual rainfall is about 50 and 250 mm in lowland and the northern highlands area, respectively. The rainfall regime in the study area is Mediterranean with hot arid summer. The maximum rainfall values are recorded in January at 15.3% annual rainfall and the minimum values are observed in December about 0.2% annual rainfall (Ahmadi, 2005). The most important land uses in the study area include: (1) rangeland and bare land (about 65%), (2) agricultural land (about 17 percent), and (3) *Haloxylon* habitats and sandy zones (about 13%).

2.2. Methods

Graphical abstract in Fig. 2 shows the full perspective of our research methodology and in the following sections we will refer to them.

2.2.1. Field sampling

In this study, two methods were used for investigation of soil quality: (1) Iranian Model of Desertification Potential Assessment (IMDPA (Ahmadi, 2005) was selected as one method to evaluate soil conditions due to its compatibility with the climatic conditions of Iran. (2) Field Manual for Local Level Land Degradation Assessment in Drylands (McDonagh and Bunning, 2009a,b) was applied because this model is up to date and has not been studied in Iran. Criteria and indicators of each method have been mentioned in Table 1.

Soil sampling was carried out by the use of stratified random sampling to create a homogeneous sampling area (Ravi et al., 2010; Salvati and Zitti, 2009) to cover more quantity and quality changes of soil. For this purpose, land use, slope, lithology, soil great group in FAO classification, and vegetation type maps were combined to create a total of 172 sampling sites. Random sampling was done at these sites and at each sampling location, in addition to measuring and scoring indices, soil samples were obtained for laboratory work and measuring indicators. Sampling and measuring started from 17 May 2012 to 8 July 2012. Then, the score of all indices and indicators were used in remote sensing modeling. It should be noted that the quantitative amount of measurable indicators (such as EC, pH, Gravel percentage and Organic carbon) was used instead of scoring due to the elimination of model error.

2.2.2. Remote sensing pre-processing and processing

According to the scope of this study, two scenarios have been used for remote sensing modeling: (1) the single-temporal: remotely sensed data were provided with samples at the same time, (2) the multi-temporal satellite data (time series): data were obtained during the year leading up to the time of sampling. In order to obtain remotely sensed data, several conditions were considered.

Many studies already show LANDSAT 4,5,7 and 8 abilities to identify soil parameters (Abdel Kawy and Belal, 2011; Abdel Kawy and Ali, 2012; El Baroudy and Moghanm, 2014; Gutierrez and Johnson, 2010; Li and Chen, 2014; Masoud, 2014; Metternicht and Zinck, 2008; Wang et al., 2013; Zhao and Chen, 2005) then in this study the TM sensor of LANDSAT 5 data were used.

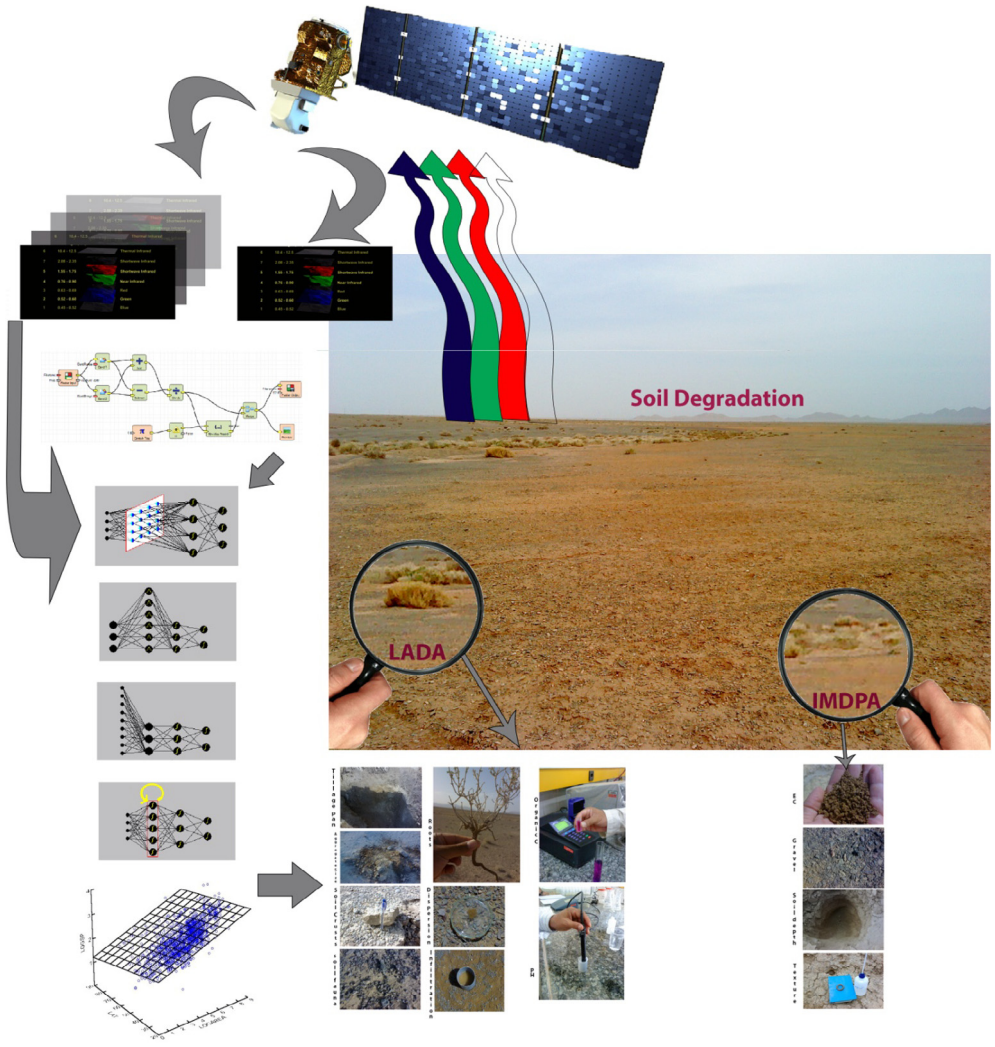

Figure 2 Graphical diagram of methodology.

(1) Images didn't have a cloud or cloud amount was less than 10 percent.Data didn't have radiometric problems such as banding, bad pixel, shot noise and multiple peaks histogram due to scattering by the atmosphere (Jensen, 2005) and at least, there weren't any regional inappropriate and unusual contrast as a result of radiometric errors in the false color composite images.
(2) There was the minimum time-lag between the time of the start and end of the sampling and date of the single-temporal remotely sensed data.
(3) To select a date in the multi-temporal scenario, the preconditions were: (a) at least, one data selects in each season (b) temporal distribution of the data is appropriate so that the data interval is not too high or low.
(4) To compare the results of two scenarios, data of two scenarios were separately modeled and single-temporal data were prevented to enter into multi-temporal data.

Finally, LANDSAT5 TM images of 22-DEC-2010, 26-APR-2010, 15-JUL-2010 and 19-OCT-2010 were selected for multi-temporal scenario and image of 31-May-2011 was selected for single-temporal scenario.

As one of the scenarios was multi-temporal, data preprocessing was performed (Jensen, 2005, 2007; Liang, 2004; Mather and Koch, 2011) to select and compare the performance of each data class data that generally eight sets of data were created and tested in the model (Table 2).

Firstly, single-temporal remotely sensed data were geometrically corrected by a GPS device and the recording of the coordinates of the points, and then the data in the other dates were registered to the single-temporal remotely sensed data (Jensen, 2005).

After geometric correction, information of each remotely sensed data sets (Table 2) was extracted in the sampling locations (172 points) to be used in a multivariate linear regression model, with all the indices and criteria soil quality and the best data sets used as input for modeling.

Also, based on the remotely sensed measurement of the parameters related to the soil, Tasseled Cap Coefficients (Li and Chen, 2014; Masoud, 2014), normalized difference bareness index (Zhao and Chen, 2005), salinity index (Wang et al., 2013), chemical and mineral composition index (Dogan, 2009), organic carbon (Huang et al., 2007), and soil humidity (Goodwin et al., 2008) were used for all dates of

Table 1 Study indices and indicators.

Model Name	Indices	Indicators	Scoring method
IMDPA	Soil	EC	Scoring to maximum EC rate in soil profile (score 0–4)
		Gravel	Scoring to gravel percent in soil profile (score 0–4)
		Texture	Scoring to predominant texture in soil profile (score 0–4)
		Soil depth	Scoring to soil depth (score 0–4)
		Total quality score	Geometric average of all indicators
LADA	Visual indicators of soil quality	Tillage pan	Scoring to Tillage pan in soil profile (score 0–2)
		Aggregate Size distribution	Scoring to Aggregate Size Distribution (score 0–2)
		Soil crusts	Scoring for either negative or positive (biological) crusts (score 0–2)
		Earthworms (or other more pertinent soil fauna)	Scoring to the presence of soil fauna in the soil (score 0–2)
		Roots	Scoring to abnormalities in root systems (score 0–2)
		Sum of visual VS-Fast scores	Sum of total weighted visual VS-Fast indicators (weights of tillage pan and Earthworms indicators:2; others: 3)
	Soil measurement indicators	Slaking and dispersion	Scoring to aggregates disintegrate in water (score 0–4)
		PH soil	Not Scored
		Water infiltration	Scoring to time of infiltration of 400 ml of water into a ring with a diameter & length of 10 cm (score 0–2)
		Organic C-labile fraction	Scoring to organic C-labile fraction using spectrophotometer (or 550 nm wavelength pocket colorimeter) based on soil texture (score 0–2)
		EC (Soil salinity)	Scoring the amount of electrical conductivity (score 0–2)
		Sum of soil measurement VS-Fast scores	Sum of total weighted soil measurement VS-Fast indicators (weights of EC and water infiltration indicators:3; organic C-labile fraction indicators: 2 and slaking and dispersion indicator:1.5)
	Sum of VS-Fast scores		Sum of VS-Fast scores

Table 2 Satellite data type used in modeling.

Satellite name	Sensor	Row	Used data	Description (Jensen, 2005; Liang, 2004; Mather and Koch, 2011)
LANDSAT 5	TM	1	Digital number	The brightness values of pixel that the sampling was done in it have been extracted
		2	Atmospheric corrected Digital Number	The atmospheric correction of digital numbers was done with dark object and regression method
		3	Radiance	Extraction of radiance values based on metadata information
		4	Illumination corrected radiance	Radiance correction based on sun angle ($\propto$) $\acute{L} = L\frac{1}{\sin(\propto)}$
		5	Terrain effect corrected radiance	By the values of slope β_t, aspect ϕ_t, Zenith angle θ_s and sun azimuth ϕ_s $L_N = \frac{Lcos(e)}{cos^k(i)cos^k(e)}$ $\cos(i) = \cos(\theta_s)\cos(\beta_t) + \sin(\theta_s)\sin(\beta_t)\cos(\phi_s - \phi_t)$
		6	Reflectance	The reflectance is obtained by the information of row 3 $\rho_p = \frac{\pi L_\lambda d^2}{ESUN_\lambda cos\theta_s}$ And for thermal band (6) $T = \frac{K2}{\ln\left(\frac{K1}{L_\lambda}+1\right)}$
		7	Illumination corrected reflectance	The reflectance is obtained by the information of row 4
		8	Terrain effect corrected reflectance	The reflectance is obtained by the information of row 5

remotely sensed data (reflectance data, row 6, Table 2) (description of soil indices in Table 3).

2.2.3. Remotely sensed modeling

2.2.3.1. Linear multivariable regression. Firstly, the data relating to the most appropriate categories (Table 2) and different soil indicators in a stepwise linear multivariable regression were entered as independent variables to model each indicator (Table 1). The analysis was separately used for each scenario (single and multi-temporal). Since increasing dimension can be costly and increases model uncertainties in the remote sensed modeling (Jensen, 2005), not only the maximum correlation coefficient of the regression model without limitation, on the number of sentences was assessed in the multivariate linear regression modeling, but also three layer models were extracted to use their parameters in nonlinear modeling to evaluate the capacity of the model in a nonlinear manner. In addition, in order to understand the influence of entering soil

Table 3 Soil evaluation indices used in this study.

Row	Indicator name	Equation	Source
1	Tasseled cap coefficients	Brightness = (0.3037 * TM1) + (0.2793 * TM2) + (0.4343 * TM3) + (0.5585 * TM4) + (0.5082 * TM5) + (0.1863 * TM7) Greenness = (−0.2848 * TM1) + (−0.2435 * TM2) + (−0.5436 * TM3) + (0.7243 * TM4) + (0.084 * TM5) + (−0.18 * TM7) Wetness = (0.1509 * TM1) + (0.1793 * TM2) + (0.3299 * TM3) + (0.3406 * TM4) + (−0.7112 * TM5) + (−0.4572 * TM7)	Li and Chen (2014), Masoud (2014)
2	Bare soil	NDBal1 = TM7 − TM6/TM7 + TM6 NDBal2 = TM5 − TM6/TM5 + TM6 NDBal3 = TM3 − TM6/TM3 + TM6	Zhao and Chen (2005)
3	Soil salinity	Salinity Index1 = TM5 − TM7/TM5 + TM7 Salinity Index2 = sqrt(TM1 × TM3)	Wang et al. (2013)
4	Mineral and chemical components	Chemical soil composition = TM5 − TM6/TM3 + TM6 Ferrous minerals = TM5/TM4 Iron oxide = TM3/TM1 Clay minerals = TM5/TM7	Dogan (2009)
5	Soil humidity	Moisture Index = TM5/TM7 Normalized difference water index = TM4 − TM5/TM4 + TM5	Goodwin et al. (2008)

quality indices (Table 3) on the regression model, the model without entry, these indices were compared with the model created by using them.

2.2.3.2. Artificial neural networks. Artificial neural networks have been used to nonlinear modeling. An artificial neural network has been entered into modern applied statistics as a reliable tool to solve many real world problems. Artificial neural network success is due to its ability to describe and model different data sets, regardless of the nature of the relationship between the data sets. In fact, artificial neural networks do not have any limitations on the use type, and they can estimate any function with any degree of complexity (Hill and Lewicki, 2006).

Artificial neural networks are the statistical tools that mimic the brain functioning. The artificial neural network is formed of a large number of neurons (nerve cells) similar to a human brain that is identified as a node or hidden units, if it receives a strong signal from another neuron to which it is connected, it transmits the message. The nature of the signal transmitted by a neuron depends on the type of function imposed on it.

In fact, nodes and neurons can be considered as a series of weakly processing units with parallel performance that each function is a mathematical function that couldn't have significant performance, but if there are appropriate numbers of them and the neurons are combined in a perfect way, they can collectively reach every goal and can build any equation (Hill and Lewicki, 2006). Therefore, the artificial neural networks can be used for statistical modeling of remotely sensed data.

Recently, great advances have been created in artificial neural network models and currently a large number of neural networks with different structures are used (Ivancevic and Ivancevic, 2005). In this study, according to Table 4 a total of 11 different models of artificial neural network were used to evaluate the increase in the accuracy of experiments using these models by NeuroSolutions 6.0 software (www.neurosolutions.com). For this purpose, instead of the result of the unrestricted multivariate linear regressions, results from confined three layer multivariate linear regressions were used to compare the performance of the two models (multivariate linear regressions and artificial neural network models in order to unwanted uncertainty were not accelerated (Jensen, 2005).

The first step, Genetic Optimization Algorithm, was used to determine the input data, momentum values, and processing elements in the hidden layer as well as number of the hidden layers of neural network model set. In this phase, the results of all the models were very similar, so separation of models in terms of performance was impossible in this way. Therefore, a key prerequisite was considered to compare the performance of each model:

(1) All models were used in the simplest case (the increase in the number of hidden layers and processing elements was avoided).
(2) The number of hidden layers in different models was considered as identical as possible (except of the Modular feed forward network that at least needed substantially two parallel hidden layers, and RBF, CANFIS and SVM had no hidden layer, a hidden layer was used for all other models).
(3) The number of processing elements in the input layer was equal to 3 and in the output layer was equal to 1. If there was a hidden layer, processing elements were considered equal to 4 in all models.
(4) In all models, exemplars were equal to 100 and the Maximum Epochs were considered 1000.
(5) In all models except the CANFIS and SVM models (because of their structure), the hyperbolic tangent was considered as a transfer function of models and learning rule was considered Levenberg-Marquardt.
(6) 30% of the samples were randomly considered as test data and 70% of them as train data (for each field model of soil degradation, once the test data were selected randomly and then the selection did not change for the indices and indicators for all the models).

Table 4 Summary of artificial neural network models used.

Row	Neural network name	Description (Ivancevic and Ivancevic, 2005)
1	Multilayer perceptrons (MLPs)	Multilayer perceptrons (MLPs) are layered feedforward networks typically trained with static backpropagation. These networks have found their way into countless applications requiring static pattern classification. Their main advantage is that they are easy to use, and that they can approximate any input/output map. The key disadvantages are that they train slowly, and require lots of training data (typically three times more training samples than network weights
2	Generalized feedforward networks	Generalized feedforward networks are a generalization of the MLP such that connections can jump over one or more layers. In theory, a MLP can solve any problem that a generalized feedforward network can solve. In practice, however, generalized feedforward networks often solve the problem much more efficiently. A classic example of this is the two spiral problem. Without describing the problem, it suffices to say that a standard MLP requires hundreds of times more training epochs than the generalized feedforward network containing the same number of processing elements
3	Modular feedforward networks	Modular feedforward networks are a special class of MLP. These networks process their input using several parallel MLPs, and then recombine the results. This tends to create some structure within the topology, which will foster specialization of function in each sub-module. In contrast to the MLP, modular networks do not have full interconnectivity between their layers. Therefore, a smaller number of weights are required for the same size network (i.e. the same number of PEs). This tends to speed up training times and reduce the number of required training examplars. There are many ways to segment a MLP into modules. It is unclear how to best design the modular topology based on the data. There are no guarantees that each module is specializing its training on a unique portion of the data
4	Jordan and Elman networks	Jordan and Elman networks extend the multilayer perceptron with context units, which are processing elements (PEs) that remember past activity. Context units provide the network with the ability to extract temporal information from the data. In the Elman network, the activity of the first hidden PEs are copied to the context units, while the Jordan network copies the output of the network. Networks which feed the input and the last hidden layer to the context units are also available
5	Principal component analysis networks	Principal component analysis networks (PCAs) combine unsupervised and supervised learning in the same topology. Principal component analysis is an unsupervised linear procedure that finds a set of uncorrelated features, principal components, from the input. A MLP is supervised to perform the nonlinear classification from these components
6	Radial basis function (RBF)	Radial basis function (RBF) networks are nonlinear hybrid networks typically containing a single hidden layer of processing elements (PEs). This layer uses gaussian transfer functions, rather than the standard sigmoidal functions employed by MLPs. The centers and widths of the gaussians are set by unsupervised learning rules, and supervised learning is applied to the output layer. These networks tend to learn much faster than MLPs.
7	Self-organizing feature maps (SOFMs)	Self-organizing feature maps (SOFMs) transform the input of arbitrary dimension into a one or two dimensional discrete map subject to a topological (neighborhood preserving) constraint. The feature maps are computed using Kohonen unsupervised learning. The output of the SOFM can be used as input to a supervised classification neural network such as the MLP. This network's key advantage is the clustering produced by the SOFM which reduces the input space into representative features using a self-organizing process. Hence the underlying structure of the input space is kept, while the dimensionality of the space is reduced
8	Time lagged recurrent networks (TLRNs)	Time lagged recurrent networks (TLRNs) are MLPs extended with short term memory structures. Most real-world data contain information in their time structure, i.e. how data change with time. Yet, most neural networks are purely static classifiers. TLRNs are the state of the art in nonlinear time series prediction, system identification and temporal pattern classification
9	Fully recurrent network	Fully recurrent networks feedback the hidden layer to itself. Partially recurrent networks start with a fully recurrent net and add a feedforward connection that bypasses the recurrency, effectively treating the recurrent part as a state memory. These recurrent networks can have an infinite memory depth and thus find relationships through time as well as through the instantaneous input space. Most real-world data contains information in its time structure. Recurrent networks are the state of the art in nonlinear time series prediction, system identification, and temporal pattern classification
10	The CANFIS (Co-Active Neuro-Fuzzy Inference System)	The CANFIS (Co-Active Neuro-Fuzzy Inference System) model integrates adaptable fuzzy inputs with a modular neural network to rapidly and accurately approximate complex functions. Fuzzy inference systems are also valuable as they combine the explanatory nature of rules (membership functions) with the power of "black box" neural networks
11	The Support Vector Machine (SVM)	The Support Vector Machine (SVM) is implemented using the kernel Adatron algorithm. The kernel Adatron maps inputs to a high-dimensional feature space, and then optimally separates data into their respective classes by isolating those inputs which fall close to the data boundaries. Therefore, the kernel Adatron is especially effective in separating sets of data which share complex boundaries. SVMs can only be used for classification, not for function approximation

(7) Each neural network model was run three times and then was repeated 10 times and the best performance was reported on the train and test data.

Because the samples were divided into two parts: training and testing data, again the multivariate linear regression models were created with these training data and then the accuracy of them were evaluated in the test data in order to compare two methods of artificial neural network and linear regression model.

3. Results

3.1. The role of data type used in performance of model

Table 4 shows the results of multivariate linear modeling using different types of remote sensed time series data. It should be noted in this table, the r column shows correlation coefficient of the regression confined to three layers, while r_{total} shows the correlation coefficient without any limitation to the number of layers. As shown in Table 5, for all criteria and indicators significant differences between the various data type functions are not seen, whether in three layer regression modeling and whether to without any limitation to numbers of layer for modeling. The only topographic corrected data often show the lower model accuracy as a result of studying most of the studied area that is flat and plain, and it could be predicted. However, this difference was not significant. Thus, although significant differences were not seen in the data type function, reflectance values (row 6, Table 2) were used according to the recommendations of additional resources (Jensen, 2005, 2007; Liang, 2004; Mather and Koch, 2011) in all subsequent stages of the study.

3.2. The role of soil quality indices

Table 6 shows the effect of the variables in the regression model. As you can see, there is no significant difference between two models with or without soil quality indices, however, when soil quality indices were used to model the Aggregate Size Distribution, Slaking and Dispersion, pH and Organic C-labile fraction indicators have a better performance (Table 6). Therefore, further statistical analyzes were allowed using the multivariate linear regression models to select inputs (either the model consists of bands or with the soil quality indices).

3.3. Linear regression modeling: time series scenarios versus single date scenario

Table 6 illustrates multi-temporal scenarios that show better performance than single-temporal in all of the criteria and indices of soil quality (except of Organic C-labile fraction using soil quality indices). Sometimes improvement of multi-temporal modeling power has been several times of single-temporal scenarios. Even in case of Slaking and Dispersion indicator related to the methodology of LADA, the time series scenario has created a predictive model, while the single-temporal scenario has not been able to make a model. An increase in the modeling power using time series data has been observed on indicators derived from laboratory and field measurements, such as EC, pH, gravel percentage and Organic C-labile fraction (in the case without the use of soil quality indices).

3.4. Artificial neural network modeling: time series scenarios versus single scenarios

The results of linear regression modeling (with layer limitation) and different types of artificial neural network models in two scenarios, single and multi-temporal, are shown in Tables 7 and 8. Firstly, the comparison between, the correlation coefficients of training data of regression modeling and artificial neural network models showed that artificial neural network models had a better performance than regression modeling in two scenarios. However, correlation coefficients of testing data did not show significant differences between the linear regression model and the best neural network model. In fact, in the complex nonlinear model of artificial neural network, only the power of training data modeling was increased, but created models did not have a good performance. Generally, artificial neural networks often have been more successful to model indicators and indices using time series data like the regression models. This better performance of time series data clearly shows correlation coefficients of train data and correlation coefficients of test data. Among the different models of artificial neural networks, Modular feed forward networks and SOFMs models in terms of correlation coefficients of train data showed the best performance. However, taking into account the correlation of test data, the best performance cannot be easily identified. However, CANFIS and RBF models are slightly better than other models.

3.5. Comparing the performance of two models

Tables 9 and 10 show correlation coefficients of linear regression using training data used in neural networks in two scenarios for this study. Correlation coefficients of test data are calculated after applying the model obtained from the train data based on test data. By comparing the correlation coefficients of the test data of Tables 9 and 10 with the test data of Tables 7 and 8, it is found that generally the performance of different models of artificial neural network is better than regression models (more in a single-temporal scenario) and power of the model in this case was more than doubled. Also, the accuracy of the train data modeling of artificial neural network is considerably higher than the linear regression models. However, the results of the multi-temporal scenario (time series data) and linear regression in most cases are not much different from the results of the best artificial neural network model. The difference between two correlation coefficients is less than 2.0 where artificial neural networks are better.

4. Conclusion

4.1. Data type

The results showed that if digital numbers are linearly preprocessed and selected remotely sensed data meet the criteria mentioned earlier (such as, without radiometric and atmospheric problems, cloud cover percent less than 10% and so on), there aren't significant differences between soil quality parameters

Table 5 comparison of linear regression performance in different data types of multi-temporal data.

Model Name	Indices	Indicators	Multivariate linear regression																			
			Digital number			Atmospheric corrected digital number			Radiance			Illumination corrected radiance			Illumination corrected reflectance			Terrain effect corrected radiance			Terrain effect corrected reflectance			Reflectance		
			Band Number & Date	r	r_{total}	Band number & date	r	r_{total}	Band number & date	r	r_{total}	Band number & date	r	r_{total}	Band number & date	r	r_{total}	Band number & date	r	r_{total}	Band number & date	r	r_{total}	Band number & date	r	r_{total}
IMDPA	Soil quality	EC	Band4_DEC Band4_APR Band5_DEC	0.623	0.708	Band4_DEC Band4_APR Band5_DEC	0.623	0.708	Band4_APR Band4_DEC Band4_JUL	0.605	0.681	Band4_DEC Band4_APR Band4_DEC	0.628	0.680	Band4_DEC Band4_APR Band5_DEC	0.639	0.698	Band4_APR Band4_DEC Band4_JUL	0.59	0.677	Band4_APR Band4_DEC Band4_JUL	0.591	0.690	Band4_DEC Band4_APR Band5_DEC	0.624	0.680
		Gravel	Band4_OCT Band5_APR Band6_APR	0.732	0.798	Band4_OCT Band5_APR Band6_APR	0.732	0.798	Band4_OCT Band5_APR Band6_APR	0.753	0.819	Band4_OCT Band5_APR Band6_APR	0.748	0.821	Band4_OCT Band5_APR Band6_APR	0.770	0.821	Band4_OCT Band5_APR Band6_APR	0.763	0.809	Band4_JUL Band6_APR Band5_APR	0.749	0.804	Band4_OCT Band5_APR Band6_APR	0.751	0.811
		Texture	Band6_APR Band4_DEC Band6_JUL	0.366	0.411	Band6_APR Band4_DEC Band6_JUL	0.366	0.411	Band6_APR Band4_DEC Band6_JUL	0.366	0.411	Band6_APR Band4_DEC Band6_JUL	0.367	0.413	Band6_APR Band4_DEC Band6_JUL	0.365	0.412	Band4_JUL Band1_APR	0.293	0.293	Band4_JUL Band1_APR	0.292	0.292	Band6_APR Band4_DEC Band6_JUL	0.364	0.410
		Soil depth	Band4_JUL Band5_DEC Band6_APR	0.552	0.570	Band4_JUL Band5_DEC Band6_APR	0.552	0.570	Band4_JUL Band5_DEC Band6_APR	0.552	0.570	Band4_JUL Band5_DEC Band6_APR	0.552	0.569	Band4_JUL Band5_DEC Band6_APR	0.551	0.568	Band4_JUL Band5_DEC Band6_APR	0.566	0.566	Band4_JUL Band5_DEC Band6_APR	0.571	0.571	Band4_JUL Band5_DEC Band6_APR	0.551	0.569
LADA	Visual indicators of soil quality	Tillage pan	Band1_DEC Band3_APR Band1_JUL	0.414	0.414	Band1_DEC Band3_APR Band1_JUL	0.414	0.414	Band1_DEC Band3_APR Band1_JUL	0.414	0.414	Band1_DEC Band3_APR Band1_JUL	0.415	0.415	Band1_DEC Band3_APR Band1_JUL	0.415	0.415	Band1_JUL Band3_APR	0.408	0.408	Band1_JUL Band3_APR	0.408	0.408	Band1_DEC Band3_APR Band1_JUL	0.414	0.414
		Aggregate Size Distribution	Band4_JUL Band3_APR Band1_APR	0.437	0.437	Band4_JUL Band3_APR Band1_APR	0.437	0.437	Band4_JUL Band3_APR Band1_APR	0.437	0.437	Band4_JUL Band3_APR Band1_APR	0.438	0.438	Band4_JUL Band3_APR Band1_APR	0.438	0.438	Band4_JUL Band3_APR Band1_APR	0.435	0.435	Band4_JUL Band3_APR Band1_APR	0.435	0.435	Band4_JUL Band3_APR Band1_APR	0.437	0.437
		Soil Crusts	Band3_DEC Band7_APR Band7_OCT	0.523	0.590	Band3_DEC Band7_APR Band7_OCT	0.523	0.590	Band3_DEC Band7_APR Band7_OCT	0.523	0.590	Band3_DEC Band7_APR Band7_OCT	0.528	0.592	Band3_DEC Band7_APR Band7_OCT	0.528	0.592	Band1_JUL Band7_APR Band7_JUL	0.517	0.540	Band1_JUL Band7_APR Band7_JUL	0.517	0.540	Band3_DEC Band7_APR Band7_OCT	0.523	0.590
		Earthworms	No Entry			No Entry			No Entry			No Entry			No Entry			No Entry			No Entry			No Entry		
		Roots	No Entry			No Entry			No Entry			No Entry			No Entry			No Entry			No Entry			No Entry		
		Sum of visual VS-Fast scores	Band1_DEC Band3_APR Band1_JUL	0.381	0.393	Band1_DEC Band3_APR Band1_JUL	0.381	0.393	Band1_DEC Band3_APR Band1_JUL	0.381	0.393	Band1_DEC Band3_APR Band1_JUL	0.383	0.395	Band1_DEC Band3_APR Band1_JUL	0.383	0.395	Band1_JUL Band3_APR	0.352	0.352	Band1_JUL Band3_APR	0.361	0.361	Band1_DEC Band3_APR Band1_JUL	0.381	0.393
	Soil measurement indicators	Slaking and Dispersion	Band2_DEC Band4_APR Band2_OCT	0.496	0.496	Band2_DEC Band4_APR Band2_OCT	0.496	0.496	Band2_DEC Band4_APR Band2_OCT	0.496	0.496	Band2_DEC Band4_APR Band3_OCT	0.477	0.549	Band2_DEC Band4_APR Band3_OCT	0.477	0.550	Band7_OCT Band6_DEC Band7_JUL	0.378	0.513	Band7_OCT Band5_DEC Band7_APR	0.349	0.466	Band2_DEC Band4_APR Band2_OCT	0.496	0.496
		pH	Band7_DEC Band5_APR Band7_OCT	0.456	0.456	Band7_DEC Band5_APR Band7_OCT	0.456	0.456	Band7_DEC Band5_APR Band7_OCT	0.456	0.456	Band7_DEC Band5_APR Band7_OCT	0.463	0.463	Band7_DEC Band5_APR Band7_OCT	0.463	0.463	Band7_JUL Band5_APR	0.402	0.402	Band7_JUL Band5_APR	0.402	0.402	Band7_DEC Band5_APR Band7_OCT	0.456	0.456
		Water Infiltration	No Entry			No Entry			No Entry			No Entry			No Entry			No Entry			No Entry			No Entry		
		Organic C-labile fraction	Band6_APR Band7_OCT Band4_JUL	0.555	0.575	Band6_APR Band7_OCT Band4_JUL	0.555	0.575	Band6_APR Band7_OCT Band4_JUL	0.555	0.575	Band6_APR Band7_OCT Band4_JUL	0.573	0.594	Band6_APR Band7_OCT Band4_JUL	0.573	0.594	Band7_JUL Band4_JUL Band3_APR	0.536	0.536	Band7_JUL Band4_JUL Band3_APR	0.535	0.535	Band6_APR Band7_OCT Band4_JUL	0.555	0.575
		Sum of soil measurement VS-Fast scores	Band1_DEC Band6_APR Band6_JUL	0.614	0.614	Band1_DEC Band6_APR Band6_JUL	0.614	0.614	Band1_DEC Band6_APR Band6_JUL	0.614	0.614	Band1_DEC Band6_APR Band6_JUL	0.611	0.611	Band1_DEC Band6_APR Band6_JUL	0.611	0.611	Band1_JUL Band3_JUL	0.478	0.478	Band1_JUL Band3_JUL	0.478	0.478	Band1_DEC Band6_APR Band6_JUL	0.615	0.615
	Sum of VS-Fast Scores	Total Score	Band1_DEC Band3_APR	0.543	0.543	Band1_DEC Band3_APR	0.543	0.543	Band1_DEC Band3_APR	0.543	0.543	Band1_DEC Band3_APR	0.538	0.538	Band1_DEC Band3_APR	0.538	0.538	Band1_JUL Band3_APR	0.473	0.473	Band1_JUL Band3_APR	0.474	0.474	Band1_DEC Band3_APR	0.543	0.543

Table 6 Performance Comparison of linear regression caused with or without the use of remote sensed indices of soil quality.

Model name	Indices	Indicators	Reflectance regression*				Model name	Indices	Indicators	Reflectance regression			
			r_{bs}	r_{is}	r_{bts}	r_{its}				r_{bs}	r_{is}	r_{bts}	r_{its}
IMDPA	Soil quality	EC	.345	.377	.68	.716	LADA	Visual indicators of soil quality	Earthworms	.00	.00	.00	.00
		Gravel	.699	.699	.811	.829			Sum of visual VS-Fast scores	.244	.340	.393	.394
		Texture	.188	.188	.410	.417		Soil measurement indicators	Slaking and dispersion	.00	.00	.496	.560
		Soil depth	.524	.527	.569	.567			Soil PH	.00	.162	.456	.555
		Total score	.281	.281	.362	.362			Water infiltration	.00	.00	.00	.00
LADA	Visual indicators of soil quality	Tillage pan	.352	.352	.414	.428			Organic C-labile fraction	.438	.624	.575	.608
		Aggregate Size Distribution	.287	.409	.437	.470			Sum of soil measurement VS-Fast scores	.433	.433	.615	.694
		Soil Crusts	.366	.366	.590	.590		Sum of VS-Fast Scores	Total score	.419	.419	.543	.546
		Roots	0.00	0.00	.00	0.00							

r_{bts}: Correlation coefficients of multi-temporal data without the use of remote sensed indices of soil quality.
r_{is}: Correlation coefficients of single-temporal data with the use of remote sensed indices of soil quality.
r_{bs}: Correlation coefficients of single-temporal data without the use of remote sensed indices of soil quality.
* r_{its}: Correlation coefficients of multi-temporal data with the use of remote sensed indices of soil quality.

modeling with digital number, and radiance and reflectance data. Only terrain effect correction preprocessing shows different results from other preprocessing due to the land slope.

4.2. The methodology of a field study of soil quality

There are two main problems to assess land degradation and desertification using remote sensing (Yang et al., 2005): (1) uncertainty field measurement and evaluation systems, (2) misuse of remotely sensed data power. Results showed that the type of field methodology and criteria and indicators has a great impact on remotely sensed modeling. Based on the findings of this research, primarily if soil quality parameters are quantitative and can be precisely measured, remotely sensed data will prove far more effective in the modeling of measurement. For example, the of gravel percentage, Organic C-labile fraction, EC and pH parameters are better than the other parameters that have been modeled due to being quantitative. Even total scores of quantitative field measurements show the capability of modeling.

4.3. Linear regression modeling

According to Table 6, the use of remote sensing indices of soil quality is not always effective, but for some indicators (such as aggregate size distribution and Organic C-labile fraction in a single temporal scenario, and pH), the use of these indices can help to increase the accuracy of modeling although these remotely sensed indices have been created from the equations conversion of the spectral bands. In other words, these indices help for the modeling of nonlinear equation, but only in special cases they are used properly. The iron oxide index is applied more than the other indices for modeling and a ferrous minerals index is the next one, and both of them identify iron compounds. According to Tables 6 and 7, the ferrous minerals index entry in Organic C-labile fraction and pH modeling increased the accuracy of modeling. These two indicators are the ratio indices that are frequently used in remotely sensed studies (Jensen, 2005), so it is recommended that in similar studies, these ratios remotely sensed indices calculated for all bands and applied for the non-linearity of the equations.

Almost for all soil quality parameters, linear regression modeling of multi-temporal scenario shows much better performance than single-temporal scenario. Although, most of the parameters examined in this study will change little during the years, but at a certain time, an indicator may show more distinction than other indices due to environmental conditions and physical–chemical construction. Therefore, it is recommended that in these studies temporal series data are used with more diversity and better distribution during the year.

4.4. Modeling by artificial neural networks

In the modeling by artificial neural network like linear regression modeling, multi-temporal scenarios have a better performance than single-temporal scenarios for both correlation coefficients of training data and correlation coefficients of testing data. It seems that in cases that the single-temporal scenario was better, repeating modeling of the multi-temporal scenario is not enough probably because the networks have the extreme local optimum (Ivancevic and Ivancevic, 2005). For example, the MLP model for multi-temporal scenarios of soil depth (Table 8) shows that it may achieve much better results by more iteration.

However, by the consideration of the correlation coefficient of training data as criteria of accuracy assessment, it seems artificial neural network models have succeeded in the modeling of all indicators and indies (whether quantitative or qualitative), but it can be generally concluded that the artificial neural networks were better in quantitative data modeling by taking into account both correlation coefficients of the training and test data. However, among the artificial neural networks, Modular feed forward networks showed the best correlation coefficient of training data, but it is noted that the model showed the weakest correlation coefficient of testing data in most iterations. Therefore, when the Modular feed forward networks used it is needed to take care and be sure to test the model. SOFMs network, similar to Modular feed forward networks, has the best correlation coefficient of train data after modular networks.

Some neural networks have shown relatively uniform and sometimes showed quite similar in different iterations. The

Table 7 Comparing the performance of different artificial neural network models and linear regression model in a single temporal scenario.

Model name	Indices	Indicators	r	Regression		Artificial neural network models																							
				Layer	Significance level	Multilayer perceptrons		Generalized feedforward networks		Modular feedforward networks		Jordan and Elman networks		Principal component analysis networks		Radial basis function		Self-organizing feature maps		Time lagged recurrent networks		Fully recurrent networks		Co-Active Neuro-Fuzzy Inference System		The Support Vector Machine	
						r_{train}	r_{test}	r_{train}	r_{test}	r_{train}	r_{test}	r_{train}	r_{test}	r_{train}	r_{test}	r_{train}	r_{test}	r_{train}	r_{test}	r_{train}	r_{test}	r_{train}	r_{test}	r_{train}	r_{test}	r_{train}	r_{test}
IMDPA	Soil Quality	EC	.42	Band4	.000	0.978	0.404	0.97	0.422	0.998	-0.355	0.92	0.56	0.84	0.283	0.7	0.211	0.98	0.322	0.8	−0.244	0.6	0.467	0.5	0.4	0.5	0.2
				NDBS2	.004																						
				Wetness	.010																						
		Gravel	.65	Band4	.000	0.87	0.60	0.89	0.69	0.99	0.64	0.92	0.64	0.88	0.64	0.82	0.62	0.99	0.57	0.96	0.5	0.82	0.58	0.79	0.5	0.72	0.39
				NDBS2	.000																						
				Clay Minerals	.003																						
		Texture	.23	Band4	.009	0.64	0.35	0.67	0.3	0.95	0.145	0.78	0.197	0.62	0.35	0.46	0.27	0.82	0.254	0.85	0.23	0.29	0.331	0.47	0.261	0.49	-0.11
				NDBS3	.103																						
		Soil depth	.52	Band4	.000	0.83	0.315	0.86	0.336	0.995	0.213	0.93	−0.207	0.8	0.207	0.69	0.354	0.98	0.309	0.92	0.323	0.74	0.473	0.61	0.455	0.81	0.254
				Band6	.001																						
				Band5	.018																						
		Total Score	.292	Band4	.000	Becuase stepwise linear regression choice just one layer, modeling by Artificial Neural Network modeling has not been done																					
LADA	Visual Indicators of Soil Quality	Tillage pan	.352	Band1	.000	Becuase stepwise linear regression choice just one layer, modeling by Artificial Neural Network modeling has not been done																					
		Aggregate Size Distribution	.409	Iron Oxide	.000	0.72	0.330	0.74	0.385	0.997	0.311	0.753	0.277	0.722	0.344	0.56	0.358	0.896	0.320	0.7	0.308	0.47	−0.328	0.65	0.333	0.88	0.232
				Band4	.001																						
		Soil Crusts	.366	Band4	.000	Becuase stepwise linear regression choice just one layer, modeling by Artificial Neural Network modeling has not been done																					
		Earthworms	0.0	No Entry		Becuase stepwise linear regression choice no layer, modeling by Artificial Neural Network modeling has not been done																					
		Roots	.202	Salinity Index1	.014	Becuase stepwise linear regression choice just one layer, modeling by Artificial Neural Network modeling has not been done																					
		Sum of visual VS-Fast scores	.340	Band1	.075	0.67	0.349	0.72	0.268	0.986	−0.328	0.788	0.299	0.71	0.349	0.53	0.336	0.88	0.263	0.66	0.331	0.44	0.192	0.486	0.302	0.69	0.315
				Iron Oxide	.004																						
				NDBS3	.026																						
	Soil Measurement Indicators	Slaking and Dispersion	0.0	No Entry		Becuase stepwise linear regression choice no layer, modeling by Artificial Neural Network modeling has not been done																					
		pH	.486	Band7	.000	0.8	0.144	0.81	0.510	0.991	0.266	0.857	0.396	0.789	0.371	0.67	0.335	0.973	0.360	0.844	0.407	0.63	0.371	0.62	0.280	0.776	0.377
				Ferrous Minerals	.000																						
				Brightmess	.000																						
		Water Infiltration	0	No Entry		Becuase stepwise linear regression choice no layer, modeling by Artificial Neural Network modeling has not been done																					
		Organic C-labile fraction	.493	Greenness	.000	0.7	0.404	0.73	0.560	0.987	0.455	0.725	0.490	0.695	0.465	0.57	0.549	0.81	0.545	0.737	0.489	0.358	0.613	0.467	0.556	0.6	−0.119
				Ferrous Minerals	.001																						
				Chemical Soil Composition	.002																						
		Sum of soil measurement VS-Fast scores	.433	Band1	.000	Becuase stepwise linear regression choice just one layer, modeling by Artificial Neural Network modeling has not been done																					
	Sum of VS-Fast Scores	Total Score	.507	Band2	.000	0.735	0.329	0.757	0.351	0.949	−0.369	0.81	0.270	0.73	0.278	0.68	0.374	0.859	0.186	0.817	0.403	0.63	0.224	0.707	0.336	0.73	0.261
				Clay Minerals	.015																						

Table 8 Comparing the performance of different artificial neural network models and linear regression model in a multi-temporal scenario.

Model name	Indices	Indicators	Regression			Artificial neural network models																					
						Multilayer perceptrons		Generalized feedforward networks		Modular feedforward networks		Jordan and Elman networks		Principal component analysis networks		Radial basis function		Self-organizing feature maps		Time lagged recurrent networks		Fully recurrent networks		Co-Active Neuro-Fuzzy Inference System		The Support Vector Machine	
			r	Layer & date	Significance level	r_{train}	r_{test}	r_{train}	r_{test}	r_{train}	r_{test}	r_{train}	r_{test}	r_{train}	r_{test}	r_{train}	r_{test}	r_{train}	r_{test}	r_{train}	r_{test}	r_{train}	r_{test}	r_{train}	r_{test}	r_{train}	r_{test}
IMDPA	Soil quality	EC	0.625	Band4_DEC Band4_APR NDBS2_DEC	.000 .000 .006	0.89	0.555	0.896	0.581	0.998	0.357	0.948	0.649	0.882	0.554	0.85	0.651	0.988	0.576	0.915	0.607	0.6	0.624	0.653	0.603	0.61	0.290
		Gravel	0.773	Band4_OCT Band5_APR Iron Oxide_JUL	.000 .000 .000	0.903	0.716	0.92	0.72	0.999	0.5	0.922	0.652	0.912	0.732	0.877	0.735	0.996	0.563	0.964	0.698	0.83	0.639	0.83	0.667	0.73	0.323
		Texture	0.364	Band6_APR Band4_DEC Band6_JUL	.000 .000 .019	0.73	0.223	0.765	−0.247	0.989	0.499	0.847	0.341	0.74	0.239	0.479	0.289	0.987	-0.312	0.923	−0.343	0.499	0.389	0.458	0.348	0.51	0.136
		Soil depth	0.549	Band4_JUL Iron Oxide_JUL Band5_DEC	.000 .001 .018	0.809	0.885	0.804	0.435	0.998	0.338	0.926	0.096	0.77	0.446	0.683	0.497	0.97	0.470	0.98	0.370	0.783	0.505	0.642	0.524	0.8	0.233
		Total score	.35	Band2_DEC	.000	Becuase stepwise linear regression choice just one layer, modeling by Artificial Neural Network modeling has not been done																					
LADA	Visual Indicators of Soil Quality	Tillage pan	0.400	Band1_DEC Iron Oxide_APR	.000 .008	0.63	0.281	0.69	0.244	0.997	0.184	0.8	0.344	0.63	0.281	0.5	0.235	0.899	0.171	0.78	0.483	0.5	0.262	0.57	0.286	0.938	0.223
		Aggregate Size Distribution	0.470	Iron Oxide_APR Band4_JUL Band4_APR	.000 .002 .040	0.77	0.454	0.786	0.495	0.998	0.413	0.84	0.374	0.764	0.453	0.66	0.425	0.963	0.297	0.69	0.445	0.47	0.313	0.643	0.508	0.876	0.459
		Soil Crusts	0.522	Band3_DEC NDBSI_APR Band7_OCT	.100 .000 .002	0.797	0.546	0.834	0.546	0.986	0.351	0.845	0.545	0.8	0.548	0.726	0.649	0.953	0.220	0.898	0.389	0.551	0.592	0.667	0.575	0.87	0.638
		Earthworms	0	No Entry		Becuase stepwise linear regression choice no layer, modeling by Artificial Neural Network modeling has not been done																					
		Roots	0.228	Clay Minerals_DEC	.005	Becuase stepwise linear regression choice just one layer, modeling by Artificial Neural Network modeling has not been done																					
		Sum of visual VS-Fast scores	0.394	Iron Oxide_APR Band7_DEC Band5_APR	.002 .000 .049	0.72	0.283	0.71	0.237	0.985	0.224	0.784	0.297-	0.73	0.207	0.55	0.1	0.925	0.315	0.69	0.266	0.576	0.189	0.153	0.160	0.714	0.146
	Soil Measurement Indicators	Slaking and Dispersion	0.516	Band2_DEC Band4_APR Greenness_OCT	.000 .000 .000	0.86	0.305	0.86	0.332	0.992	-0.169	0.848	-0.175	0.857	0.150	0.7	0.337	0.913	0.187-	0.926	0.287	0.647	0.317	0.7	0.431	0.830	0.241
		pH	0.519	Ferrous Minerals_DEC Salinity Index1_OCT Wetness_DEC	.000 .000 .003	0.847	0.229	0.849	0.311	0.994	0.263	0.895	0.390	0.847	0.348	0.774	0.415	0.979	0.152	0.845	0.290	0.69	0.356	0.740	0.329	0.794	0.313
		Water Infiltration	0	No Entry		Becuase stepwise linear regression choice no layer, modeling by Artificial Neural Network modeling has not been done																					
		Organic C-labile fraction	0.567	Greenness_APR Band6_JUL Ferrous Minerals_JUL	.000 .001 .002	0.876	0.589	0.864	0.596	0.997	0.445	0.878	0.516	0.798	0.588	0.7	0.536	0.978	0.368	0.845	0.616	0.57	0.618	0.674	0.670	0.63	0.283
		Sum of soil measurement VS-Fast scores	0.620	Band1_DEC Band6_APR Moisture Index_OCT	.000 .000 .000	0.793	0.364	0.824	0.363	0.992	0.222	0.852	0.433	0.8	0.359	0.68	0.494	0.960	0.268	0.842	0.517	0.69	0.541	0.715	0.553	0.753	0.315
	Sum of VS-Fast Scores	Total Score	0.546	Band1_DEC NDBS3_APR	.000 .001	0.732	0.370	0.759	0.352	0.958	0.273	0.86	0.301	0.837	0.322	0.7	0.403	0.817	0.509	0.824	0.273	0.7	0.171	0.71	0.378	0.75	0.454

Table 9 Results of linear regression modeling of training data of artificial neural network models in single-temporal scenario.

Model name	Indices	Indicators	Regression Reflectance			Model name	Indices	Indicators	Regression Reflectance		
			Layer	r_{train}	r_{test}				Layer	r_{train}	r_{test}
IMDPA	Soil Quality	EC	Band4	0.422	0.2	LADA	Visual Indicators of Soil Quality	Aggregate Size Distribution	Iron Oxide Band4	0.420	0.364
			NDBS2 Wetness					Sum of visual VS-Fast scores	Band1 Iron Oxide NDBS3	0.318	0.270
		Gravel	Band4	0.708	0.499						
			NDBS2 Clay Minerals				Soil Measurement Indicators	pH	Band7	0.182	0.164
		Texture	Band4	0.235	0.230				Ferrous Minerals Brightmess		
			NDBS3								
		Soil depth	Band4	0.540	0.494			Organic C-labile fraction	Greenness	0.387	0.565
									Ferrous Minerals Chemical Soil Composition		
			Band6								
							Sum of VS-Fast Scores	Sum of soil measurement VS-Fast scores	Band2	0.484	0.223
			Band5						Clay Minerals		

SVM model is more stable than all other models, and it does not need to repeat. After that, CANFIS network showed the most consistency in various iteration, and PCA and RBF were in next stability. The MLP models and models derived from it indicated very different results of modeling in various repeats. Therefore, it is suggested that enough repeats are used to make high sure before the end of the modeling by these networks (see soil depth indicator in multi-temporal scenario of Table 8).

Using of Genetic algorithm was tried after achieving the preliminary results of artificial neural network models, the parameters of each network are optimized for soil quality indicators modeling, but the results showed that in spite of a significant increase in the correlation coefficient of training data, the correlation coefficient of testing data is at the same level of previous modeling. In fact, remotely sensed prediction of soil parameters based on existing data did not show the capability of increasing the power of modeling with this method.

It may be thought that the increase of input dimension can strengthen the artificial neural network models. However, as Jensen (2005) noted, test uncertainty costs also went up with an increase in the input dimension (an increase in data-input to more than three-layers). The scientific analysis was examined for some quantitative indices such as organic carbon, gravel, EC and pH, and it was observed that if the entrance dimension into the artificial neural network is similar to the output of stepwise linear regression, correlation coefficient shows a considerable reduction in the test data, in spite of significant increase in training data correlation coefficients.

Actual comparison of linear regression modeling and artificial neural networks to the training and testing data (Tables 9 and 10) showed that, although relationships between remotely sensed data may be nonlinear in many cases (Jensen, 2007) modeling accuracy won't increase dramatically by using nonlinear artificial neural networks. However, based on the comparison of the numbers of Tables 7 and 9 it can be recommended artificial neural networks modeling is better than linear modeling such as regression modeling in single-temporal scenarios. However, these networks cannot be recommended by comparing Tables 8 and 10 due to the complexity of neural networks and uncertain data that will be created. In fact, actual accuracy of the two modeling in multi-temporal scenario (regression and best model of neural network) is close to each other (exception of PH). In this case, multi-temporal nonlinear methods such as nonlinear remote sensed indices are preferred.

4.5. Suggestions for further researches

Desertification affects different types of environments thus any decision focusing on desertification requires deep research on the characteristics of the area under analysis (Santini et al., 2010). This paper is concerned with exploring an alternative remotely sensed approach for assessing the soil degradation. The procedure focuses on different criteria of two field based methods of soil degradation assessment. This study shows that quantitative indicators of these two models can be modeling properly by remotely sensed data. However, LADA Methodology is preferred because some of its indicators can be measured by hands or portable Laboratory tools (indicators of soil measurement VS-Fast scores criteria), it is possible to

Table 10 Rresults of linear regression modeling of training data of artificial neural network models in multi-temporal scenario.

Model name	Indices	Indicators	Regression Reflectance			Model name	Indices	Indicators	Regression Reflectance			Model Name	Indices	Indicators	Regression Reflectance		
			Band number & date	r_{train}	r_{test}				Band number & date	r_{train}	r_{test}				Band number & date	r_{train}	r_{test}
IMDPA	Soil Quality	EC	Band4_DEC	0.691	0.609	LADA	Visual Indicators of Soil Quality	Tillage pan	Band1_DEC	0.401	0.336	LADA	Soil Measurement Indicators	pH	Ferrous Minerals_DEC	0.278	0.063
			Band4_APR						Iron Oxide_اردیبهشت						Salinity		
			Band5_DEC					Aggregate Size Distribution	Iron Oxide_APR	0.506	0.439				Index1_OCT		
									Band4_JUL						Wetness_DEC		
									Band4_APR					Organic C-labile fraction	Greenness_APR	0.477	0.572
		Gravel	Band4_OCt	0.734	0.708			Soil Crusts	Band3_DEC	0.510	0.481				Band6_JUL		
									NDBS1_APR						Ferrous Minerals_JUL		
									Band7_OCT								
			Band5_APR					Sum of visual VS-Fast scores	Iron Oxide_APR	0.463	0.170			Sum of soil measurement VS-Fast scores	Band1_DEC	0.661	0.576
									Band7_DEC								
									Band5_APR						Band6_APR		
			Band6_APR				Soil Measurement Indicators	Slaking and Dispersion	Band2_DEC	0.563	0.368						
		Texture	Band6_APR	0.337	0.336										Moisture Index_OTC		
			Band4_DEC										Sum of VS-Fast Scores	Total Score	Band1_DEC	0.589	0.432
			Band6_JUL						Band4_APR								
		Soil depth	Band4_JUL	0.596	0.366										NDBS3_APR		
			Band5_DEC						Greenness_OCT								
			Band6_APR														

collect these data in field directly and there is no limitation to use in other countries. But modified models of ESAs such as IMDPA are region-based. We must point out both models lack the setting that is needed for remote sensing analysis and further researches must be done to combine different indicators of soil degradation that are suitable for use in remotely sensed data. Gravel percentage, Organic C-labile fraction, EC, pH, Slaking and Dispersion, and Soil Crusts are indicators that have the potential to be used in this new model.

Conflict of interest

The authors declare no conflict of interest.

References

Abdel Kawy, W.A.M., Ali, R.R., 2012. Assessment of soil degradation and resilience at northeast Nile Delta, Egypt: the impact on soil productivity. Egypt. J. Remote Sens. Space Sci. 15 (1), 19–30.

Abdel Kawy, W.A., Belal, A.-A., 2011. Soil resilience mapping in selective wetlands, West Suez Canal, Egypt. Egypt. J. Remote Sens. Space Sci. 14 (2), 99–112.

Ahmadi, H., 2005. The final report of compiling a comprehensive service plan and methodology of indicators and indices of desertification potential assessment in Iran, College of Agriculture & Natural Resources, Faculty of Natural Resources, Department of Rehabilitation of Arid and Mountainous Regions, University of Tehran.

Bouaziz, M., Matschullat, J., Gloaguen, R., 2011. Improved remote sensing detection of soil salinity from a semi-arid climate in Northeast Brazil. C.R. Geosci. 343 (11–12), 795–803.

Cammeraat, L.H., Imeson, A.C., 1998. Deriving indicators of soil degradation from soil aggregation studies in southeastern Spain and southern France. Geomorphology 23, 307–321.

de Paz, J.M., Sanchez, J., Visconti, F., 2006. Combined use of GIS and environmental indicators for assessment of chemical, physical and biological soil degradation in a Spanish Mediterranean region. J. Environ. Manage. 79 (2), 150–162.

Diodato, N., Ceccarelli, M., 2004. Multivariate indicator Kriging approach using a GIS to classify soil degradation for Mediterranean agricultural lands. Ecol. Ind. 4 (3), 177–187.

Dogan, H.M., 2009. Mineral composite assessment of Kelkit River Basin in Turkey by means of remote sensing. J. Earth Syst. Sci. 118 (6), 701–710.

Douaoui, A.E.K., Nicolas, H., Walter, C., 2006. Detecting salinity hazards within a semiarid context by means of combining soil and remote-sensing data. Geoderma 134 (1–2), 217–230.

El Baroudy, A.A., Moghanm, F.S., 2014. Combined use of remote sensing and GIS for degradation risk assessment in some soils of the Northern Nile Delta, Egypt. Egypt. J. Remote Sens. Space Sci. 17 (1), 77–85.

FAO/UNEP, 1983. Provisional Methodology for Assessment and Mapping of Desertification. F2624. FAO.

Feoli, E., Vuerich, L.G., Zerihun, W., 2002. Evaluation of environmental degradation in northern Ethiopia using GIS to integrate vegetation, geomorphological, erosion and socio-economic factors. Agric. Ecosyst. Environ. 91, 313–325.

Geist, H.J., Lambin, E.F., 2004. Dynamic causal patterns of desertification. Bioscience 54 (54), 817–829.

Ghadiry, M., Shalaby, A., Koch, B., 2012. A new GIS-based model for automated extraction of Sand Dune encroachment case study: Dakhla Oases, western desert of Egypt. Egypt. J. Remote Sens. Space Sci. 15 (1), 53–65.

Goodwin, N.R., Coops, N.C., Wulder, M.A., Gillanders, S., Schroeder, T.A., Nelson, T., 2008. Estimation of insect infestation dynamics using a temporal sequence of Landsat data. Remote Sens. Environ. 112 (9), 3680–3689.

Gutierrez, M., Johnson, E., 2010. Temporal variations of natural soil salinity in an arid environment using satellite images. J. S. Am. Earth Sci. 30 (1), 46–57.

Haijiang, L., Chenghu, Z., Weiming, C., En, L., Rui, L., 2008. Monitoring sandy desertification of Otindag Sandy Land based on multi-date remote sensing images. Acta Ecologica Sinica 28 (2), 627–635.

Helldén, U., Tottrup, C., 2008. Regional desertification: a global synthesis. Global Planet. Change 64 (3–4), 169–176.

Hill, T., Lewicki, P., 2006. Statistics: Methods and Applications: A Comprehensive Reference for Science, Industry, and Data Mining. StatSoft, Tulsa, OK.

Hill, J., Stellmes, M., Udelhoven, T., Röder, A., Sommer, S., 2008. Mediterranean desertification and land degradation. Global Planet. Change 64 (3–4), 146–157.

Huang, X., Senthilkumar, S., Kravchenko, A., Thelen, K., Qi, J., 2007. Total carbon mapping in glacial till soils using near-infrared spectroscopy, Landsat imagery and topographical information. Geoderma 141 (1–2), 34–42.

Ibáñez, J., Valderrama, J.M., Puigdefábregas, J., 2008. Assessing desertification risk using system stability condition analysis. Ecol. Model. 213 (2), 180–190.

Ivancevic, V.G., Ivancevic, T.T., 2005. Natural Biodynamics. World Scientific, Hackensack, N.J..

Jauffret, S., Visser, M., 2003. Assigning life-history traits to plant species to better qualify arid land degradation in Presaharian Tunisia. J. Arid Environ. 55 (1), 1–28.

Jensen, J.R., 2005. Introductory digital image processing: a remote sensing perspective. In: Prentice Hall Series in Geographic Information Science, third ed. Prentice Hall, Upper Saddle River, N.J..

Jensen, J.R., 2007. Remote sensing of the environment: an earth resource perspective. In: Prentice Hall Series in Geographic Information Science, second ed. Pearson Prentice Hall, Upper Saddle River, NJ..

Kosmas, C., Kirkby, M., Geeson, N., 1999. The Medalus project Mediterranean desertification and land use: Manual on key indicators of desertification and mapping environmentally sensitive areas to desertification, European Commission.

Ladisa, G., Todorovic, M., Trisorio Liuzzi, G., 2012. A GIS-based approach for desertification risk assessment in Apulia region, SE Italy. Phys. Chem. Earth Parts A/B/C 49, 103–113.

Li, S., Chen, X., 2014. A new bare-soil index for rapid mapping developing areas using LANDSAT 8 data. ISPRS – International Archives of the Photogrammetry, Remote Sensing and Spatial Information Sciences, XL-4, 139–144.

Liang, S., 2004. Quantitative remote sensing of land surfaces. In: Wiley Series in Remote Sensing. Wiley-Interscience, Hoboken, N.J..

Liu, Y., Gao, J., Yang, Y., 2003. A holistic approach towards assessment of severity of land degradation along the Greatwall in Northern Shaanxi Province, China. Environ. Monit. Assess. 82, 187–202.

Masoud, A.A., 2014. Predicting salt abundance in slightly saline soils from Landsat ETM + imagery using Spectral Mixture Analysis and soil spectrometry. Geoderma 217–218, 45–56.

Mather, P.M., Koch, M., 2011. Computer Processing of Remotely-Sensed Images: An Introduction, fourth ed. Wiley-Blackwell, Chichester, West Sussex, UK, Hoboken, NJ.

McDonagh, J., Bunning, S., 2009a. Field Manual for Local Level Land Degradation Assessment in Drylands, LADA-L Part 1: Methodological Approach. FAO, Planning and Analysis, pp. 76.

McDonagh, J., Bunning, S., 2009b. Field Manual for Local Level Land Degradation Assessment in Drylands, LADA-L Part 2: Local Assessment: Tools and Methods for Fieldwork. FAO, p. 133.

Metternicht, G., Zinck, A., 2008. Remote Sensing of Soil Salinization: Impact on Land Management. CRC Press.

Okin, G.S., Parsons, A.J., Wainwright, J., Herrick, J.E., Bestelmeyer, B.T., Peters, D.C., Fredrickson, E.L., 2009. Do changes in connectivity explain desertification? Bioscience 59 (3), 237–244.

Omuto, C.T., 2008. Assessment of soil physical degradation in Eastern Kenya by use of a sequential soil testing protocol. Agric. Ecosyst. Environ. 128 (4), 199–211.

Pinet, P.C., Kaufmann, C., Hill, J., 2006. Imaging spectroscopy of changing Earth's surface: a major step toward the quantitative monitoring of land degradation and desertification. C. R. Geosci. 338, 1042–1048.

Rasmussen, K., Fog, B., Madsen, J.E., 2001. Desertification in reverse? Observations from northern Burkina Faso. Global Environ. Change 11, 271–282.

Rasmy, M., Gad, A., Abdelsalam, H., Siwailam, M., 2010. A dynamic simulation model of desertification in Egypt. Egypt. J. Remote Sens. Space Sci. 13 (2), 101–111.

Ravi, S., Breshears, D.D., Huxman, T.E., D'Odorico, P., 2010. Land degradation in drylands: interactions among hydrologic–aeolian erosion and vegetation dynamics. Geomorphology 116 (3–4), 236–245.

Rodríguez, A.R., Mora, J.L., Arbelo, C., Bordon, J., 2005. Plant succession and soil degradation in desertified areas (Fuerteventura, Canary Islands, Spain). Catena 59 (2), 117–131.

Ruiz-Sinoga, J.D., Diaz, A.R., 2010. Soil degradation factors along a Mediterranean pluviometric gradient in Southern Spain. Geomorphology 118 (3–4), 359–368.

Salvati, L., Zitti, M., 2009. Assessing the impact of ecological and economic factors on land degradation vulnerability through multiway analysis. Ecol. Ind. 9 (2), 357–363.

Santini, M., Caccamo, G., Laurenti, A., Noce, S., Valentini, R., 2010. A multi-component GIS framework for desertification risk assessment by an integrated index. Appl. Geogr. 30 (3), 394–415.

Sha-Sha, F., Pei-Jun, L., Qian, F., Xiao-Jun, L., Peng, L., Yue-Bing, S., Yang, C., 2011. Soil quality degradation in a magnesite mining area. Pedosphere 21 (1), 98–106.

Snakin, V.V., Krechetov, P.P., Kuzovnikova, T.A., Alyabina, I.O., Gurov, A.F., Stepichev, A.V., 1996. The system of assessment of soil degradation. Soil Technol. 8, 331–343.

Stocking, M., Murnaghan, N., 2000. A Handbook for the Field Assessment of Land Degradation. Routledge, Norwich.

Wang, Z., Daun, C., Yuan, L., Rao, J., Zhou, Z., Li, J., Yang, C., Xu, W., 2010. Assessment of the restoration of a degraded semi-humid evergreen broadleaf forest ecosystem by combined single-indicator and comprehensive model method. Ecol. Eng. 36 (6), 757–767.

Wang, F., Chen, X., Luo, G., Ding, J., Chen, X., 2013. Detecting soil salinity with arid fraction integrated index and salinity index in feature space using Landsat TM imagery. J. Arid Land 5 (3), 340–353.

Yanda, P.Z., 2000. Use of soil horizons for assessing soil degradation and reconstructing chronology of degradation processes: the case of Mwisanga Catchment, Kondoa, central Tanzania. Geomorphology 34, 209–225.

Yang, X., Zhang, K., Jia, B., Ci, L., 2005. Desertification assessment in China: an overview. J. Arid Environ. 63 (2), 517–531.

Zhao, H., Chen, X., 2005. Use of Normalized Difference Bareness Index in Quickly Mapping Bare Areas from TM/ETM+. In: International Geoscience & Remote Sensing Symposium, IGARSS. IEEE Seoul, Korea, pp. 1666–1668.

Zucca, C., Biancalani, R., Hamrouni, H., Attia, R., Bunning, S., 2009. Guidelines for the identification, selection and description of nationally based indicators of land degradation and improvement. LADA, p. 57.